



# IJRASET

International Journal For Research in  
Applied Science and Engineering Technology



---

# INTERNATIONAL JOURNAL FOR RESEARCH

IN APPLIED SCIENCE & ENGINEERING TECHNOLOGY

---

**Volume:** ICAAA-2018 **Issue:** Conference **Month of publication:** April 2018

**DOI:**

[www.ijraset.com](http://www.ijraset.com)

Call:  08813907089

E-mail ID: [ijraset@gmail.com](mailto:ijraset@gmail.com)

# Computational Investigation of Rear Spoiler of a Car

Sujith S Menon<sup>1</sup>, Thamizhselvan.R<sup>2</sup>, Rajivgandhi S<sup>3</sup>

<sup>1,2</sup> Student, Institute of Industrial Design, Chennai, India

<sup>3</sup>Senior Application Engineer, Institute of Industrial Design, Chennai, India

**Abstract:** Spoilers are basically installed in a car so that the lift force can be avoided, get better traction control, improve handling, reduce drag force, create a laminar flow of air and it also improves the mileage of the car. Spoilers in a car are different from the wings of an airplane. The wings in an airplane are used to achieve lift but spoilers in a car are used to get better traction control. This paper focuses on computing the effects of rear spoiler on a car using CATIA V5 for designing and ANSYS FLUENT 18.1 for analysis. Also we observe the drag co-efficient  $C_D = 0.00083279$  and maintaining the down force as per the standards which is less than existing car drag force.

**Keywords:** Rear Spoiler; NACA4512; CFD; Drag Co-efficient; Downforce

## I. INTRODUCTION

A spoiler is an automotive aerodynamic device which is mainly utilized to 'spoil' unfavorable air movement across a moving vehicle body, usually described as turbulence or drag. Spoilers on the front of a vehicle are often called air dams. A rear spoiler is used to change the flow of air on the rear end of the vehicle. Spoilers were first introduced on vehicles in the late 1960's and used on sports and racing cars in the 1970's [1]. Today spoilers are used in almost each and every single car. They are of unique styles and designs but most drivers use it for alternate reasons such as reducing drag force, reducing lift and increase traction control. The benefits of installing a car spoiler will be maintaining traction, increasing fuel efficiency, added visibility, reduce weight, increase braking stability and also give the car a stylish look. Cars travelling at high speeds tend to create a lift, spoilers can create a down force to counteract the lift and give the car more stability.

The spoilers are classified as Pedestal spoiler, Front spoilers, Lip spoilers and Wings. Pedestal spoilers are the type of spoilers found on the rear of car or on the top of the trunk which provides more stability. Front spoilers also known as air dams are used in the front to reduce the drag created by rear spoilers and block unstable airflows from entering the chassis. Lip spoilers are smaller and sleeker than regular rear spoilers used for aesthetics and reducing lift. Wings are large rear spoilers used on race cars to create a down force to stabilize the car at high speeds. In the past rear spoilers on a car caught on as a fashion statement but today they play a much bigger role in vehicle dynamics. With the introduction of active spoilers they have gone a step forward, An active spoiler is one which dynamically adjusts while the vehicle is in operation based on conditions presented, changing the spoiling effect, intensity or other performance attribute.

The effects of air flow over the spoilers can be calculated using flow based analytical equations. Computational fluid dynamics (CFD) gives a detailed and accurate solution than when the calculation is done theoretically [1-5]. Computational methods give better predictions in a short time. It basically formulates on the continuity equation energy equation and the momentum equation.

## II. PROBLEM DEFINITION

Cars travelling at higher Speeds have a tendency to lift over. The flow of air at the rear end of the car tends to create a pressure drop which it initiates the lift, a rear spoiler can be attached to the car to reduce this lift [1,3,4]. The objective of this paper is to investigate the effect of flow over the rear spoiler at a speed of 126.94m/s (457km/h, top speed of Koenigsegg Agera RS). As cars today are breaking top speed records and manufacturers are trying to come up with super cars that can reach much higher speeds, stability of the car and the aerodynamic flow is of great importance. So the characteristics of rear spoilers at high speeds need to be computed.

## III. METHODOLOGY

Fluid flow analysis is packed with problems to be solved. In the past the numerical problems used to be carried out by hand and desk calculators later it was carried out by digital computers. Computerized Calculations made it easier to analyze the design and gave faster outputs and results. It also gave more accurate results than manually calculated results.

A. Analytical

It mainly deals with the theoretical part of the calculations, the governing equations and its relevant formulae used in solving the problem. Analytical method of calculation is time consuming and accurate for simple problems like cantilever etc .The governing equations of fluid flow represents mathematical statements of conservation laws of physics.

- 1) The mass of a fluid is conserved [8], Equation (1).
- 2) The rate of change of momentum equals the sum of forces on the fluid particle (Newton’s second law) [9], Equation (2).
- 3) The rate of change of energy is equal to the sum of rate of heat addition and the rate of work done on a fluid particle (First law of thermodynamics) [8], Equation (3).

$$\frac{\partial \rho}{\partial t} + \text{div}(\rho \mathbf{u}) = 0 \tag{1}$$

$$\frac{\partial \mathbf{u}}{\partial t} + (\mathbf{u} \cdot \nabla) \mathbf{u} = -\frac{1}{\rho} \nabla p + \nu \nabla^2 \mathbf{u} \quad , \nabla \cdot \mathbf{u} = 0 \tag{2}$$

$$\begin{aligned} \rho \frac{DE}{Dt} = & -\text{div}(\rho \mathbf{u}) + \left[ \frac{\partial(u\tau_{xx})}{\partial x} + \frac{\partial(u\tau_{yx})}{\partial y} + \right. \\ & \left. \frac{\partial(u\tau_{zx})}{\partial z} + \frac{\partial(v\tau_{xy})}{\partial x} + \frac{\partial(v\tau_{yy})}{\partial y} + \frac{\partial(v\tau_{zy})}{\partial z} + \right. \\ & \left. \frac{\partial(w\tau_{xz})}{\partial x} + \frac{\partial(w\tau_{yz})}{\partial y} + \frac{\partial(w\tau_{zz})}{\partial z} \right] + \\ & \text{div}(k \text{ grad } T) + S_E \end{aligned} \tag{3}$$

B. CFD

CFD is a methodology for obtaining a discrete solution for real world fluid problems; this solution is obtained at a finite collection of space points at a certain intervals of time. This computational analysis only possible through high speed computers and the analysis of the flow problem is done using ANSYS fluent. This process is a simulation based design and analyses instead of the normal build and test method. The Build and test method of analysis is very time consuming and waste of production capital. CFD techniques have been used in aerospace industry since the 1960’s in design, manufacturing of aircraft and jet engines[8]. Further now they have been used in the design and manufacture of internal combustion engines and is being widely used in automotive industry.

CFD codes are structured around numerical algorithms that can tackle fluid flow problems. These codes contain three main elements:

- 1) Pre-processor
- 2) Solver
- 3) Post-processor

IV. COMPUTATIONAL DOMAIN AND MESH GENERATION

The rear spoiler was designed using 3D designing software CatiaV5. The airfoil design used in the rear spoil design is of NACA 4512 coordinates as shown in Figure 1.The four-digit string containing the NACA airfoil code. The first digit is the amount of camber in units of 1% of the chord length. The second digit is the location of maximum camber measured from the leading edge in units of 10% of the chord length. The final two digits are the thickness of the airfoil in units of 1% of the chord length. Advantages of 4 digit airfoils are they provide Good stall characteristics, Small centre of pressure movement across large speed range, Roughness has little effect. These are the ones most commonly used for designing horizontal tails and in general aviation.

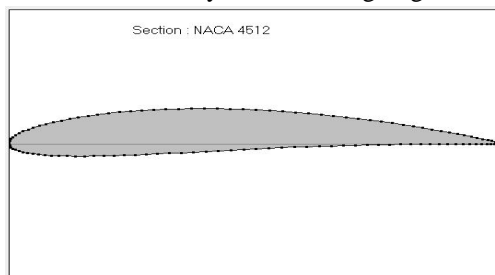


Figure 1. NACA 4512 airfoil cross-section.

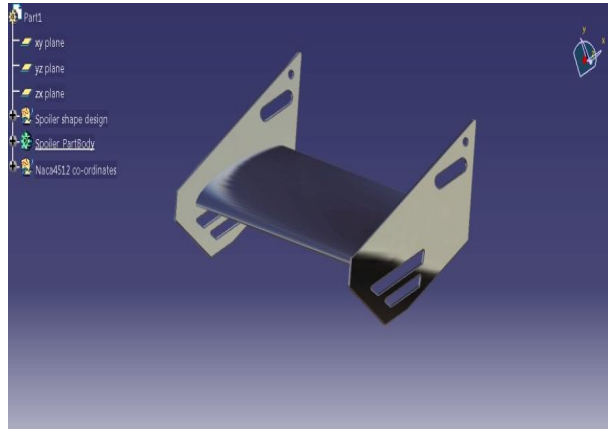


Figure 2. Rear Spoiler CATIA design.

The enclosure for external fluid flow is created with SAE standards. The dimensions from the origin were given as +x direction 32.197m, -x direction 17.172m, +y direction 3.360m and -y direction 3.360m. The CATIA design geometry is shown in Figure 2. For discretization of the computational domain the body is generated into polyhedral type mesh as shown in Figure3.

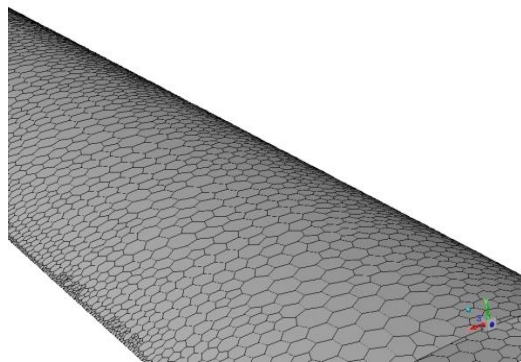


Figure 3. Polyhedral mesh surface of spoiler.

### V. NUMERICAL AND COMPUTATIONAL ANALYSIS

The force on the vehicle in the direction opposite to its moving direction is called drag Equation 4, and the force perpendicular to the drag and normal to the ground is called lift, Equation 5. The higher the drag force is, the more the horsepower is required. The drag and lift forces can be expressed in a non-dimensional form the drag and lift coefficients,  $C_D$  and  $C_L$ , are defined respectively as

$$C_D = \frac{Drag}{(\rho V^2 A)/2} \tag{4}$$

$$C_L = \frac{Lift}{(\rho V^2 A)/2} \tag{5}$$

Where  $\rho$  is the air density,  $V$  is the vehicle velocity;  $A$  is the frontal projected area of the vehicle [3].

The co-efficient of pressure ( $C_p$ ) is the difference between local static pressure and free-stream (at  $\infty$ ) static pressure, non dimensionalized by the free-stream dynamic pressure, Equation 6. At any point in the flow where the local pressure coefficient  $C_p$  is defined as

$$C_p = \frac{P - P_\infty}{P_T - P_\infty} \tag{6}$$

$C_p$ , at the airfoil stagnation point, is unity[10].

**VI. BOUNDRY CONDITIONS AND SETUP PROCEDURE.**

*A. Model*

In the model task page, for analysis of external flow the viscous model is set to Spalart-Allmaras equation. This model design was basically used for aerospace applications and is found to give better results for boundary layers subjected to high pressure gradients. This is one equation model that evaluates based on the kinematic eddy viscosity (turbulent flow). The SA viscous model is a low Reynolds number model and it is able to resolve the flow field down to the solid wall. It gives a more accurate result in the external flow analysis. The advantage of the SA model equation is that it is very stable and shows good convergence.

*B. Material*

The material of the fluid flow is set to air with ideal gas properties.

*C. Boundary Conditions*

The problem consists of flow around the spoiler body at different angles of attack ( $\alpha$ ) therefore certain boundary conditions are provided. The enclosure domain set around the spoiler body is set as the pressure farfield due to the external flow of air around the spoiler body and variations in pressure needs to be computed. As the speed of spoiler is 126.94m/s and the speed of sound in the medium is 340m/s so the resultant Mach number is 0.37. Thus the Mach number for the pressure farfield zone is set as 0.37. The flow is computed for different angles of attack and the x-component is given as  $\cos \alpha$  and y-component is given as  $\sin \alpha$  based on each value of  $\alpha$ , the z-component is always 0.

*D. Solution Methods*

The problem at hand is a pressure based solver problem the pressure velocity coupling needs to be enabled and the algorithm for the solution method needs to be set. As the flow problem is not that complicated and the fluid flow is in steady state conditions we can set the pressure velocity coupling to the default SIMPLE(Semi-Implicit method for pressure linked equation) method. In spatial discretization the default least square cell based gradient is retained and rest all are set to second order upwind. Upwind schemes represent different numerical techniques to solve the hyperbolic partial differential equations and second order upwind provides a better technique of solving than first order upwind.

*E. Solution Controls*

The values for each factors controlling the solution outcome is set in solution controls as given in Table 1.

TABLE 1. Solution Controls

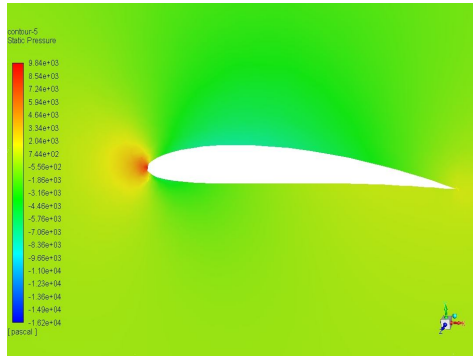
SL no:	Under Relaxation Factors	
	Factors	Values
1	Pressure	0.3
2	Density	1
3	Body forces	1
4	Momentum	0.7
5	Modified Turbulent Viscosity	0.8
6	Turbulent Viscosity	1
7	Energy	1

**VII. RESULTS AND DISCUSSION**

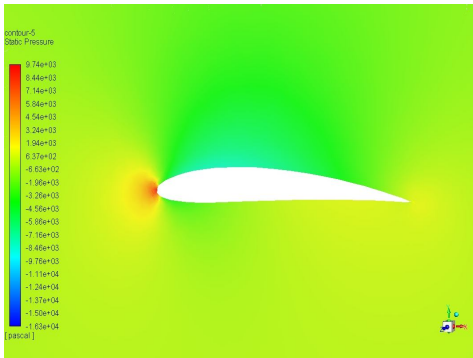
The resultant contours are shown in the figures below. In these figures the red region indicates the highest magnitude of pressure or velocity magnitude and the blue region depicts the lesser magnitudes. Within the scale the variations of both pressure and velocity magnitudes are shown by the varying colours of yellow and green.

*A. Contours of Pressure Magnitude*

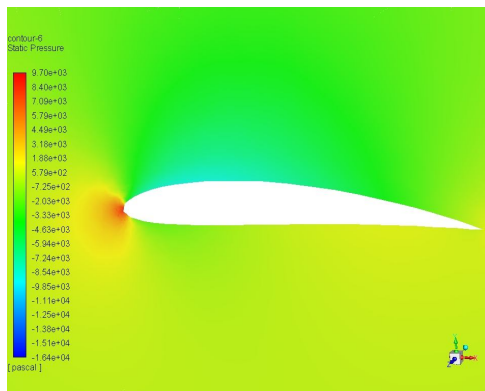
The variations in pressure magnitude for various angle of attack can be observed from the contour images as shown in the below Figure 5. Also the highest pressure region can also be observed.



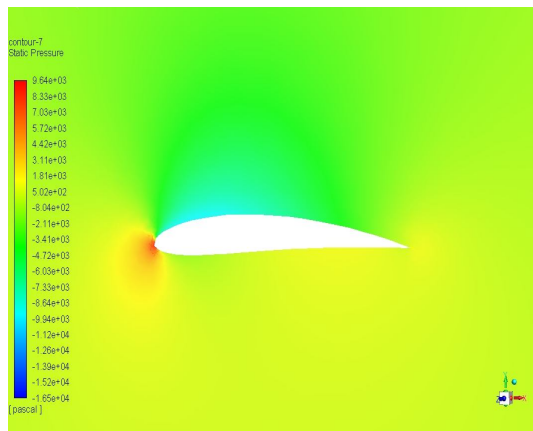
(a)



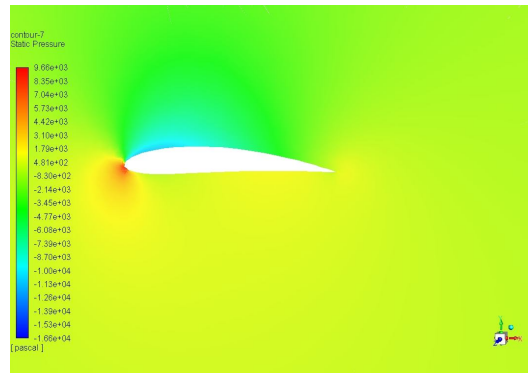
(b)



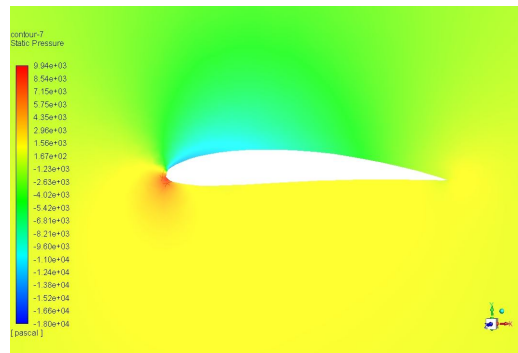
(c)



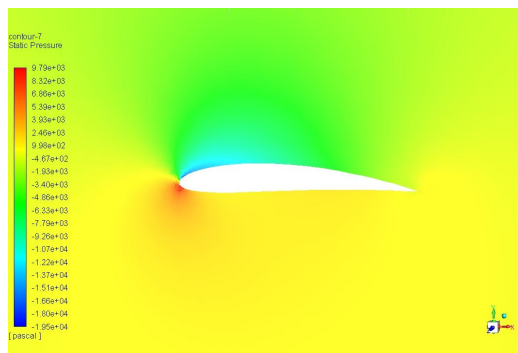
(d)



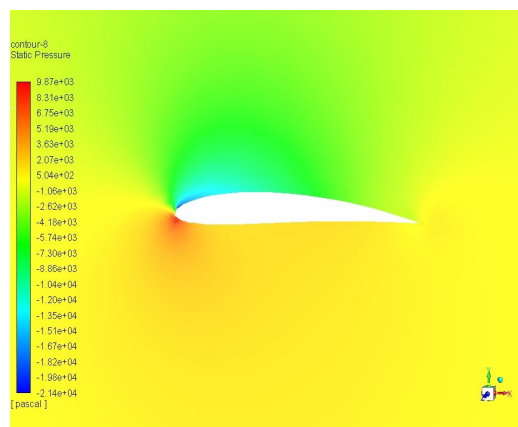
(e)



(f)



(g)

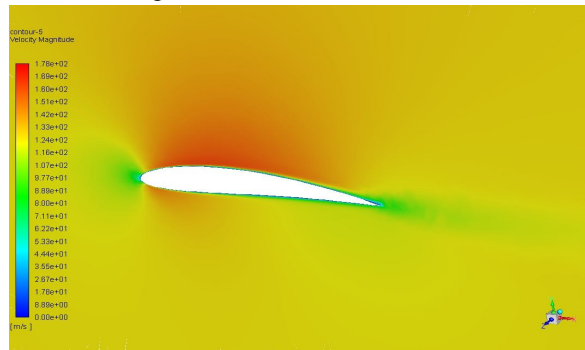


(h)

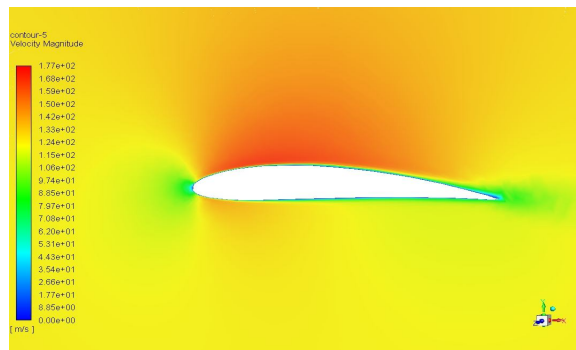
Figure 5. The figure (a) to (h) shows the pressure magnitude contours for the angles of attack  $0^{\circ}$  to  $7^{\circ}$  respectively.

**B. Contours for velocity Magnitude**

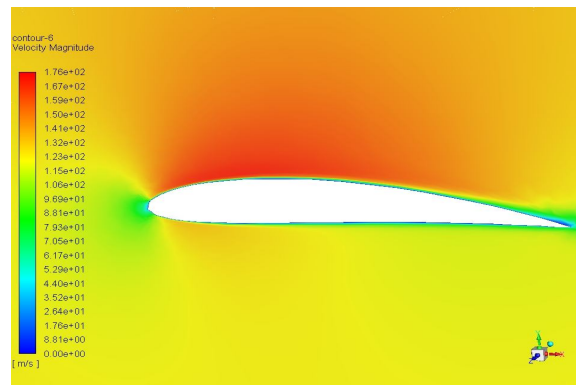
The variations in the velocity magnitude for each angle of attack can be observed from the contour images given below in Figure 6.



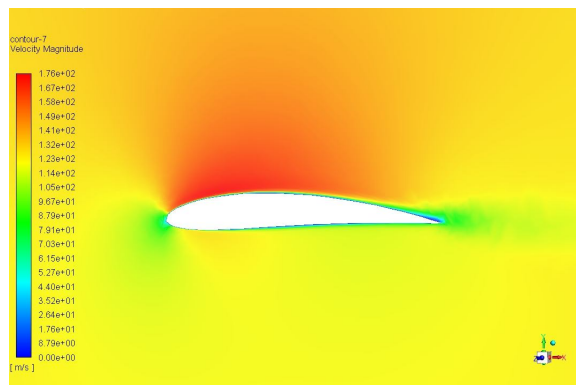
(a)



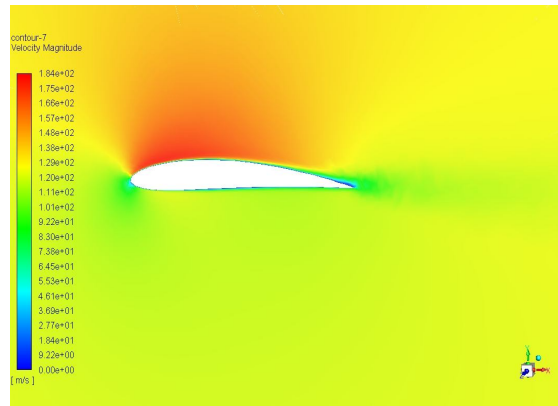
(b)



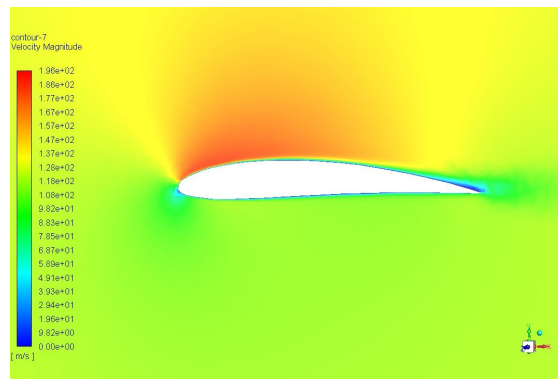
(c)



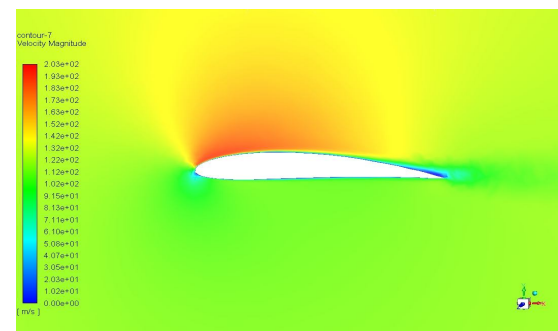
(d)



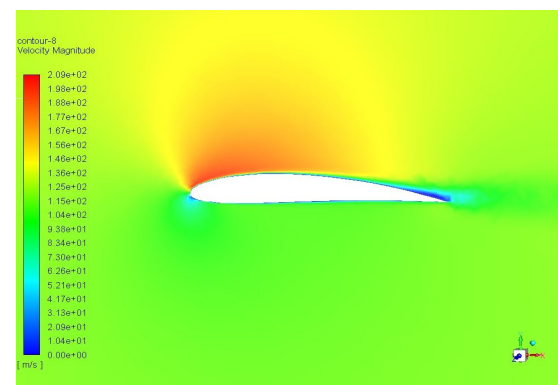
(e)



(f)



(g)

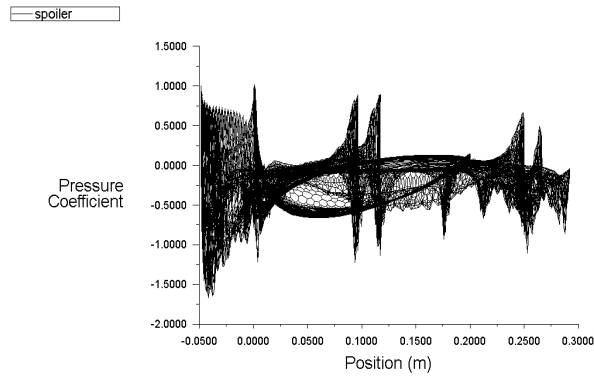


(h)

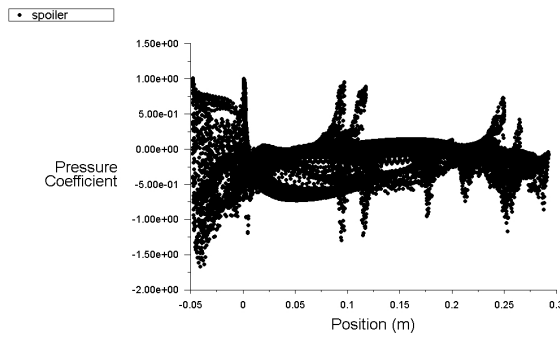
Figure 6. The figure (a) to (h) shows the velocity magnitude contours for the angles of attack  $0^{\circ}$  to  $7^{\circ}$  respectively.

C. Cp Plots For different angle of attack

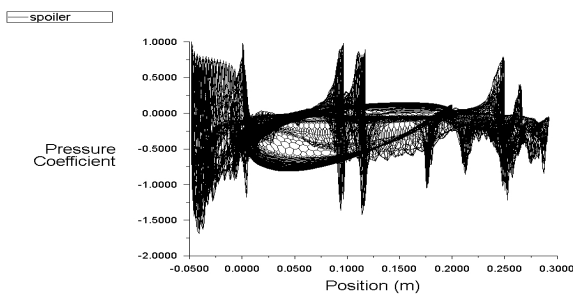
The pressure co-efficient ( $C_p$ ) at different positions on the spoiler is plotted in a XY plot showing the variations of pressure co-efficient along the spoiler body.



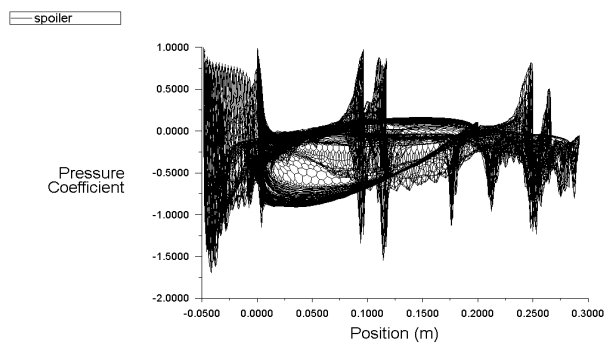
(a)



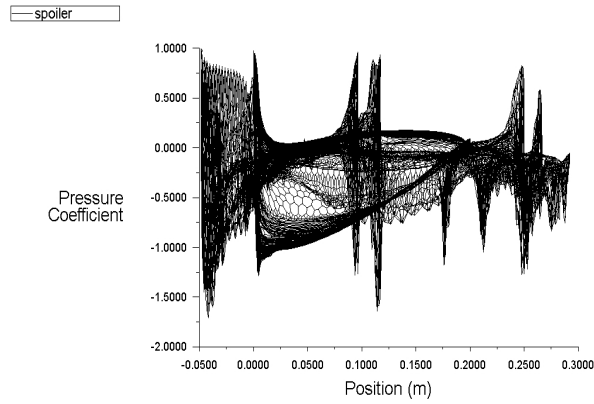
(b)



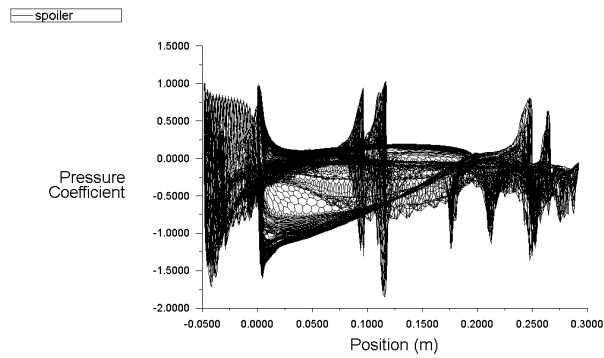
(c)



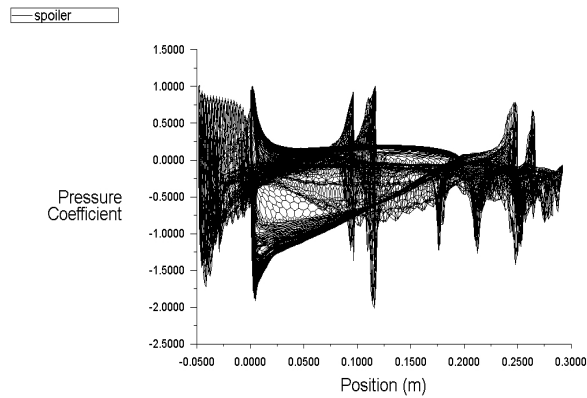
(d)



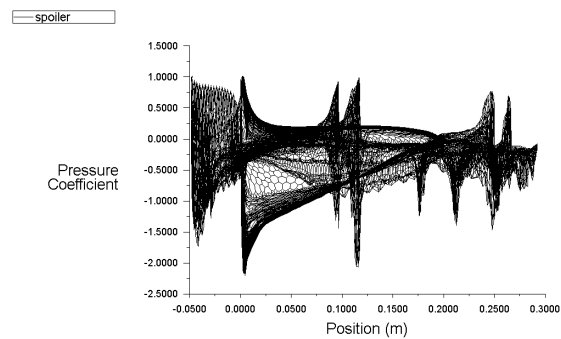
(e)



(f)



(g)



(h)

Figure 7. The XY plots (a) to (h) show the variations of  $C_p$  along the Y-axis and the positions along the X-axis for different angles of attack  $\alpha$  from  $0^\circ$  to  $7^\circ$  respectively.

TABLE 2. Te results for the respective coefficients and forces for each angle of attack  $\alpha$ .

Sl no:	Angle of attack( $\alpha$ )	$C_D$	$C_L$	$C_P$	Pressure Forces(N)	Viscous Forces(N)
1.	$0^\circ$	0.005344	0.069279	0.003713086	36.028239	15.824691
2,	$1^\circ$	0.0042803	0.08701	0.004098098	39.764024	16.452497
3.	$2^\circ$	0.0027999	0.10466	0.004702583	45.629376	16.865808
4.	$3^\circ$	0.00083279	0.12231	0.005478291	53.156105	17.018768
5.	$4^\circ$	-0.0015493	0.13939	0.006437007	62.458566	16.882529
6.	$5^\circ$	-0.0043175	0.15564	0.007552891	73.286034	16.59533
7.	$6^\circ$	-0.0073601	0.17076	0.008865746	86.024725	16.125629
8.	$7^\circ$	-0.010314	0.18399	0.010423322	101.13795	15.481026

From the above Table 2 it can be observed that the lift co-efficient, pressure co-efficient and pressure forces increases as the angle of attack increases. But it can be observed that the viscous forces increases till  $3^\circ$  then starts decreasing . Similarly it can be observed that the drag co-efficient decreases as the angle of attack increases but after  $3^\circ$  angle of attack the drag coefficient is negative which results in more lift. Hence the angle  $3^\circ$  can be observed as the optimum angle of attack resulting in the optimum values of  $C_D$ ,  $C_L$ ,  $C_P$ , pressure force and viscous force. The XY plots of the resultant values are plotted. Figure 8 shows the graph between the drag coefficient and the lift coefficient. Figure 9 shows the graph plotted between the angle of attack and the drag coefficient similarly the graph between the angle of attack and lift co-efficient is plotted in Figure 10.

D.  $C_D$  v/s  $C_L$  Plot

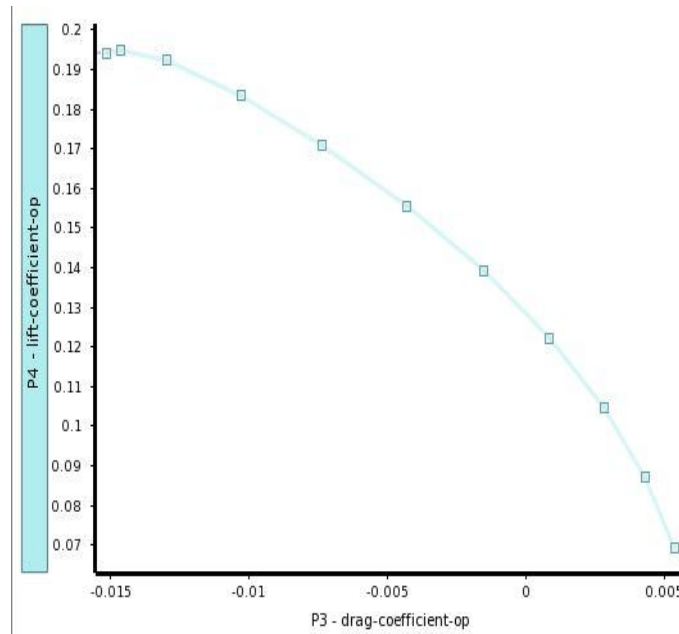


Figure 8. XY plot showing drag coefficient  $C_D$  along x axis and drag coefficient  $C_L$  the y axis.

E. Angle of attack  $\alpha$  v/s  $C_D$

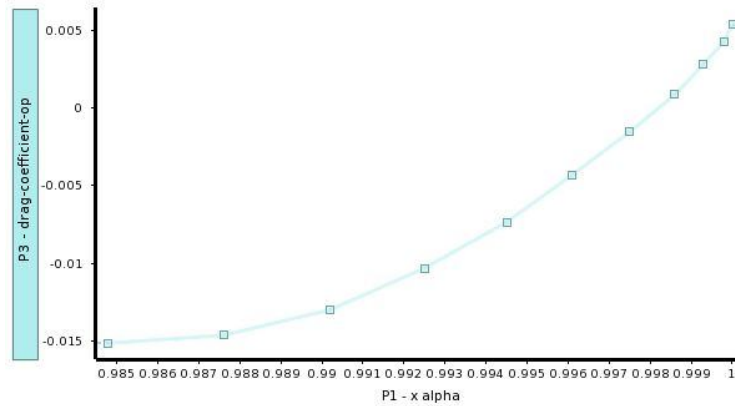


Figure 9. XY plot showing angle of attack  $\alpha$  along the x axis and drag coefficient  $C_D$  along y axis.

F. Angle of attack  $\alpha$  v/s  $C_L$

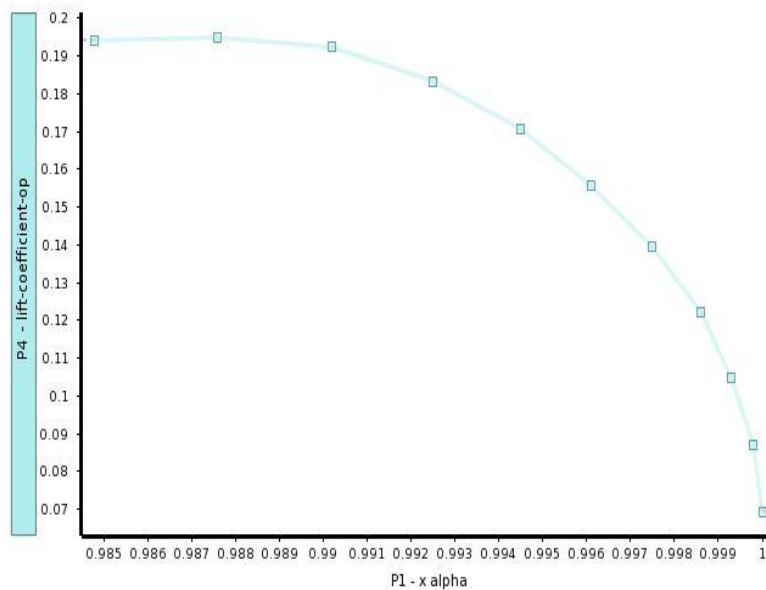


Figure 10 . XY plot showing angle of attack  $\alpha$  along the x axis and drag coefficient  $C_L$  along y axis.

VIII. CONCLUSION

As per the result and discussion of external flow dynamics of spoiler explained about the safer angle of attack (3 to 4 degree) is observed with appropriate pressure distribution, velocity contours and pressure coefficient plot with respect to the chord. And also plotted the coefficient of lift and drag ( $C_D=0.00083$  &  $C_L=0.1228$ ) values, relevant pressure coefficient, pressure force over the spoiler and viscous force are 0.005478291, 53.156105N, and 17.018768N which is optimum when compared with the standard cp plot as shown in figure. The future enhancement of this spoiler is to be study and investigate about deformation and stress distribution. Also it will be helpful for the next generation vehicles.

IX. ACKNOWLEDGMENT

We thank Lord Almighty for guiding us in every step towards the completion of our project. We are thankful to Mr. Midhun Lal H. Application Engineer, Institute of Industrial Design, Chennai, India for his guidance and support. We extend our deep gratitude to our project guide, Rajivgandhi S, Senior Application Engineer, Institute of Industrial Design, Chennai, India for his careful and meticulous reviews which improved the quality of this work. We truly admire our parents for their constant encouragement and their enduring support which has been inevitable for the success of our ventures.

## REFERENCES

- [1] Sandy Minkah Kyei Composite Car Rear Spoiler ,Degree Thesis, Plastics Technology,2014
- [2] Syed Fahad Anwer Fluid Mechanics Group Department of Mechanical Engineering Aligarh Muslim University, Aligarh, Introduction to Computational Fluid Dynamics Computational Methods in Engineering Applications IIT Kanpur, 12-16 April 2016
- [3] Xu-xia Hu, Eric T.T. Wong ,A Numerical Study On Rear-spoiler Of Passenger Vehicle, World Academy of Science, Engineering and Technology International Journal of Mechanical and Mechatronics Engineering Vol:5, No:9, 2011
- [4] Naveen Kumar, K. Lalit Narayan, L. N. V. Narasimha Rao and Y. Sri Ram, Investigation of Drag and Lift Forces over the Profile of Car with Rear spoiler using CFD V, Mechanical Engineering, Sir. C.R. Reddy College of Engineering, Andhra Pradesh, India International Journal of Advances in Scientific Research 2015; 1(08): 331-339.
- [5] R. B. Sharma<sup>1</sup>, Ram Bansal<sup>2</sup>, Aerodynamic Drag Reduction of a Passenger Car Using Spoiler with VGs, International Journal of Engineering Research and Applications (IJERA) ISSN: 2248-9622 International Conference On Emerging Trends in Mechanical and Electrical Engineering (ICETMEE- 13th-14th March 2014).
- [6] T. J. CHUNG , COMPUTATIONAL FLUID DYNAMICS University of Alabama in Huntsville
- [7] Fluid mechanics by FM White
- [8] Computational fluid dynamics by Mallasekara
- [9] Dan S. Henningson Martin Berggren, Fluid Dynamics: Theory and Computation, August 24, 2005.
- [10] Mohamed A. Fouad Kandil\* , Abdelrady Okasha Elnady, Performance of GOE-387 Airfoil Using CFD, International Journal of Aerospace Sciences 2017, 5(1): 1-7.
- [11] Dr. M.V. Sathish Kumar<sup>1</sup>, B. Ashwin Rao<sup>2</sup>, Dr. g. Mallaiiah<sup>3</sup>, Design, Analysis and Manufacturing of a Car Rear Spoiler for Drag Reduction, IARJSET, Vol 4, Issue 6, June 2017.
- [12] G. Ganesh, V. Vasudevan, Analysis of Effects of Rear Spoiler in Automobile using Ansys, International Journal of Scientific & Engineering Research, Volume 6, Issue 6, June 2015, ISSN 2229-5518



10.22214/IJRASET



45.98



IMPACT FACTOR:  
7.129



IMPACT FACTOR:  
7.429



# INTERNATIONAL JOURNAL FOR RESEARCH

IN APPLIED SCIENCE & ENGINEERING TECHNOLOGY

Call : 08813907089  (24\*7 Support on Whatsapp)